

*" The therapeutic effect of thymoquinone on methotrexate induced ovarian toxicity in adult female albino rats "*

Authors

[Fatma Aلسedik Nabih](#)<sup>1</sup>, [Ehab Abdel Aziz Ahmed El-Shaarawy](#)<sup>2</sup>, [Heba Youssef](#)<sup>3</sup>,  
[Abd Elrahman Elshahat](#)<sup>4</sup>, [Sarah M. Mowafy](#)<sup>5</sup>

<sup>1</sup> Human anatomy and embryology

<sup>2</sup> Professor of Anatomy and Embryology Department Faculty of Medicine  
(Kasr Alainy), Cairo University

<sup>3</sup> Forensic Medicine and Clinical Toxicology Department Faculty of Medicine, Port Said  
University

<sup>4</sup> Assistant Professor of Anatomy and Embryology, Faculty of Medicine, Port Said  
University

<sup>5</sup> Lecturer of Anatomy and Embryology, Faculty of Medicine, Port Said University

Submitted: 08/10/2024

Accepted: 12/10/2024

DOI: 10.21608/muj.2024.326910.1190

ISSN : 2682-2741

This is an open access article licensed under  
the terms of the Creative Commons  
Attribution International License (CC BY 4.0).

<https://muj.journals.ekb.egdean@med.psu.edu.eg>  
[vice\\_dean\\_postgraduate@med.psu.edu.eg](mailto:vice_dean_postgraduate@med.psu.edu.eg)



**ABSTRACT:**

Background: Methotrexate is an antineoplastic drug in the treatment of many morbidities. Besides its various benefits, it may induce hazardous effects on different body systems. One of its collateral impacts is ovarian toxicity. Oxidative stress and inflammation are suggested to play a main role in methotrexate induced toxicity. Thymoquinone, a natural agent, is nowadays widely used in the medical field due to its antioxidant, and excellent anti-inflammatory nature as well as its anti apoptotic .effect

Aim: This study aimed to assess the protective role of thymoquinone in different .doses in defiance of methotrexate ovarian toxicity

Material and method: 36 rats were randomized and divided into 6 groups, 6 rats in each. Group I: received no treatment. Group II: received 0.5 mL saline for 11 days. Group III: Methotrexate was received in a single 20 mg/kg dose. Group IV, V and VI: received methotrexate as group III and thymoquinone in doses of 2.5, 5 and 10 mg/kg/day respectively for 11 days. Levels of MDA, SOD, TNF $\alpha$  and AMH were measured. Histopathological and immunostaining examinations with caspase 3 were .done

Results: Group III showed significantly elevated of MDA and TNF $\alpha$  levels and lower levels of SOD and AMH in contrary to the control groups. Groups V and VI showed obvious improvement in the biochemical results. Ovarian sections in group III showed degenerated follicles, disrupted granulosa cells degenerated corpora lutea and intense caspase3 immunopositivity. The normal histology of the ovary was restored .with negative immunostaining of caspase 3 in groups V and VI

Key words: methotrexate, ovary, oxidative stress, thymoquinone

## **INTRODUCTION**

Methotrexate (MTX), a folic acid antagonist, is used widely in treating many morbidities. **(Bajas et al., 2021)**. It is used for diverse types of cancers such as cancers of the lung, breast, osteosarcoma, choriocarcinoma, non-Hodgkin's lymphoma, leukemia, tumors of head and neck as well as tumors of the ovary. Being developed originally as an anti-cancer agent, MTX is now considered the gold standard and the first choice of anti-rheumatic drugs in the treatment of many autoimmune inflammatory disorders mainly rheumatoid arthritis, vasculitis, juvenile idiopathic arthritis, and psoriasis as well as multiple sclerosis, systemic lupus erythematosus, inflammatory bowel disorders, **(Bedoui et al., 2019)**. It has distinct methods of action when used in treating cancers. In cancer, MTX acts as a competitive inhibitor of the formation of purine and pyrimidine of both DNA and RNA **(Makhaylov et al., 2019)**. Furthermore, its polyglutamate inhibits the neo-synthesizing of purine and thymidylate synthase, thus decreasing DNA formation as a result, especially in rapidly dividing cells **(Singh et al., 2019)**.

MTX exerts its anti-inflammatory action via increasing endogenous adenosine release, reducing cell proliferation, influencing the production of cytokines, increasing apoptosis of T cells, and alteration of expression of cellular adhesion molecules **(Cronstein & Aune, 2020)**.

Significant toxicity to multiple body systems, including the reproductive, blood, digestive tract, liver, kidney, and central nervous system, has been reported with MTX **(Hafez et al., 2021; Gunyeli et al., 2021 and Zhao et al., 2023)**.

Oxidative stress (OS) participates in the tissue damage implied by MTX. Intracellularly, MTX is retained in the cytosol as polyglutamate MTX which accumulates intracellularly when used for a long period, leading to folic acid reduction and inhibition of cytosolic (NADP)-dependent dehydrogenases that lead to decreased (NADPH) which is used to maintain glutathione, avital cytosolic antioxidant. Consequently, lowering of the antioxidant enzymes inside the cells converting them to reactive oxygen species. **(Madkour et al., 2022)**.

Besides, MTX induces lipid peroxidation as evidenced by a marked rise of malondialdehyde (MDA). Lipid peroxidation is the principle cause of cell membrane damage. In addition, MTX raises nitric oxide synthase (iNOS) activity leading to NO increased concentration resulting in oxidative tissue injury. **(El-Fatah and Alsemeh, 2019 and Zaki et al., 2021)**.

MTX affects the female reproductive tract centered on its antifolate effects exerted on all rapidly dividing cells, thus it could produce ovarian dysfunction. High dose MTX damages the ovarian follicles causing a reduction in their numbers **(Hortu et al., 2020)**.

**Aka et al., 2022** stated that the method of ovarian toxicity of MTX is oxidative stress which is confirmed by the rise of MDA concentrations which reflects cell membrane lipid peroxidation causing severe damage in the cell. **Also, Madkour et al., 2022** reported that the main proposed causes responsible for MTX toxicity are OS, inflammation, and apoptosis.

Natural compounds have recently gained interest as conceivable medicinal compounds for ameliorating the toxic effects of different anti-cancer drugs. One of these herbs, *Nigella sativa* is an annual herbaceous plant that has Thymoquinone (TQ) as its major bioactive component. TQ exposes a wide scope of biological and therapeutic potentials including antioxidant, , antidiabetic, antibacterial, antitussive, antihypertensive, anticancer, antiapoptotic, and anti-inflammatory effects **(Farooq et al., 2021)**.

Due to its powerful antioxidant activity against several ROS, including OH radicals, superoxide anion, and singlet oxygen, TQ can ameliorate the damaging effects resulting from elevated ROS in different diseases **(Tabassum et al., 2021)**.

Former studies documented the beneficial effects of TQ in mitigating some male and female reproductive systems disorders (**Yaghutian Nezhad et al., 2021**). TQ exhibited a protective effect by hindering ROS from destroying germ cells in the rat gonads maintaining the integrity of germ cells and thus increasing the concentration of gametes (**Alabdullah et al., 2020**).

Furthermore, TQ improved the hormonal and histomorphological parameters, increased normal folliculogenesis, and markedly decreased cyst formation in the ovaries by provoking the antioxidant system and limiting cellular apoptosis. (**AL-ghamdi et al., 2023 and Patel et al., 2023**).

TQ was able to reduce tissue damage and alleviate ischemia/reperfusion injury on ovaries at various developmental stages by exhibiting its protective and therapeutic action through antioxidant and anti-inflammatory effects via increasing catalase and glutathione peroxidase activity and decreasing MDA and interleukin-6 (IL-6) concentrations (**Colluoglu et al., 2022**).

While MTX-induced ovarian toxicity presents a major challenge for women of reproductive age receiving treatment, researching natural therapies like TQ may help to mitigate these toxic effects and enhance patient outcomes.

## **2. Materials and methods**

### **2. 1. Chemicals**

MTX from Hikma Specialized Pharmaceuticals, (Badr City, Cairo, Egypt), TQ was obtained from Acro's Organics, (Belgium, China),. Caspase 3 rabbit polyclonal antibodies were persuaded out of Thermo Fisher Scientific Inc. /Lab Vision (Fremont, CA, USA).

### **2. 2. Experimental animals**

The study was established following the ethical policies and procedures of Animal Ethical Committee of the Faculty of Medicine, Port Said University. ERN; MED (1/11/2022) s.no (60) ANA800-001. Thirty-six adult female Albino rats 150-250 grams were supplied by the Animal House of the Faculty of Science, Port Said University, Egypt. Rats were accommodated in wire-fencing enclosures at ambient temperature, where laboratory food and tap water were freely available. Rats were given 2 weeks to become accustomed before the experiment began.

### **2. 3. Experimental design**

Rats were arranged into 6 groups evenly in this manner:

Group (I) (Negative control): Rats did not receive any treatment throughout the experiment.

Group (II) (Positive control): Each rat received 0.3 mL of 0.9% saline through intraperitoneal injection (IP) for 11 days.

Group (III) (MTX group): Each rat was injected with a single dose of IP MTX (20 mg/kg body weight) (**Gunyeli Saygin, and Ozmen 2021**).

Group (IV) (MTX + TQ1): Rats took MTX as in group (III) and was injected with TQ in 2.5 mg /kg/ day dose IP for 11 days (**Mehri et al. 2014**).

Group (V) (MTX + TQ2 group): Each rat received MTX as in group (III) and was injected with TQ in 5 mg/kg/day dose IP for 11 days (**Mehri et al. 2014**).

Group (VI) (MTX + TQ3 group): Each rat received MTX as in group (III) and was injected with TQ in 10 mg /kg/day dose IP for 11 days (**Mehri et al. 2014**).

## **2.4. Sample collection:**

Rats received phenobarbital 40 mg/kg body weight through IP injection twelve hours after the end of the experiment. (Laferriere & Pang, 2020). Rats were slaughtered, ovaries were dissected, and blood sampling was obtained through cardiac aspiration and centrifuged at 4000 rpm for twenty minutes to measure level of superoxide dismutase, Malondialdehyde, tumor necrosis factor-alpha, and anti-Mullerian hormone (AMH). Samples were frozen at -20°C till assayed.

## **2.5. Biochemical analysis**

### **2.5.1. Measurement of serum Malondialdehyde (MDA) level:**

MDA assessment depended on spectrophotometric readings of the formed pink compound at a wavelength of 532 nm and 95°C by MDA and thiobarbituric acid. (Kei, 1978) using kits purchased from Bio Diagnostic, (Giza, Egypt). Levels were represented as nmol/m.

### **2.5.2. Measurement of serum superoxide dismutase (SOD) level:**

The potential of SOD enzyme for preventing the reduction of nitro blue tetrazolium dye was the principle of the Colorimetric way that was used to measure SOD, as stated by Nishikimi et al. in 1972. An absorbance change over 5 minutes at 560 nm was linked to an inhibition rate which is directly related to SOD activity. The SOD level is represented as U/mg hemoglobin, where U is the SOD quantity needed for impeding 50% reduction of nitro blue tetrazolium dye. Kits supplied by Bio Diagnostic, (Giza, Egypt).

### **2.5.3. Measurement of serum tumor necrosis factor-alpha (TNF- $\alpha$ ) level:**

Detection of TNF- $\alpha$  was done via ELISA kits based on the instructions of the manufacturer (Bio Legend, San Diego, California, United States). ON a 96-well plate, Armenian hamster monoclonal rat TNF- $\alpha$ -specific antibody was coated on, To produce an antibody-antigen-antibody reaction, an anti-rat TNF- $\alpha$  detection antibody, biotinylated goat polyclonal antibody, was added. Avidin-horseradish peroxidase was compined generating a blue color. Then, the color changed to yellow by adding a stop solution, and levels were read at 450 nm (Mammadov et al., 2019).

### **2.5.4. Measurement of serum AMH levels:**

Using Chemiluminescent Immunoassay (CLIA) kits supplied by Mindray Bio-Medical Electronics Co. (China), which is a two-site sandwich assay where samples, Ra and Rb were added., AMH could be bound to the reagents to form a sandwich complex. Then, anti-AMH antibody alkaline phosphatase catalyzed substrate solution. The final response was analyzed automatically. The results were shown in the unit of ng/mL (Wang et al., 2022).

## **2. 6. Histopathological analysis:**

ovarian tissues were subjected to a graded alcohol solution after being infused in a 10% NBF, cleaned in xylene, embedded in paraffin wax ,and then under a light microscope provided with a digital camera (BX53F, Olympus, Tokyo, Japan), 5  $\mu$ m H&E-dyed cuts were evaluated.

## **2. 7. Immunohistochemical examinations:**

Using the streptavidin-biotin method, the ovarian sections were immuno-stained with rabbit polyclonal anti-caspase-3 antibody by the streptavidin-biotin technique. After a 60-minute incubation period with a primary antibody, a streptavidin–alkaline phosphatase conjugate and Histostain SP kit (LAB-SA system, Zymed Laboratories Inc, San Francisco, CA 94080, USA) were combined. using DAB as a chromogen, the antigens were assessed.

## 2. 8. Statistical analysis

The results were evaluated through SPSS 20 (Statistical Program for Social Science, version 20) and were interpreted as means  $\pm$  SD. Bonferroni post-hoc test following one-way ANOVA test was applied to analyze group differences. Statistically significant results were set at  $p < 0.05$ .

## 3. Results

### 3. 1. Biochemical results

Levels of MDA, an oxidative stress indicator, were significantly higher in group III contrary to the control groups. Meanwhile, treatment with TQ markedly decreased MDA levels in groups V & VI compared to group III. However, MDA levels in group IV were significantly higher than in the control groups, but still significantly reduced opposite to group III. (**Table 1**).

The presence of the inflammation process in our study was evident by significant elevation of TNF- $\alpha$  levels in group III in contrary to control groups. TQ in 5 & 10 mg/kg doses could mitigate the inflammatory process and significantly dampen the level of TNF- $\alpha$  in serum. Giving TQ in 2.5 mg/kg dose caused no significant alteration in TNF- $\alpha$  levels in serum in contrast to the MTX group. (**Table 1**).

MTX caused a prominent decrease in levels of SOD and AMH in group III when compared with control groups. Yet, SOD and AMH levels increased in groups V&VI versus group III. However, the increase in SOD and AMH levels of group IV was insignificant contrary to group III. (**Table 1**).

### 3. 2. Hematoxylin & Eosin results

Upon light microscopic examination, the control group's ovarian sections displayed the characteristic histological structure, where the germinal epithelium was made up of one layer of cuboidal or flat cells covering the surface and the underlying tunica albuginea. The ovary is formed of an outer cortex and inner medulla. The cortex exhibited different types of follicles, within a stroma densely packed with cells. The inner medulla showed Lymph and blood vessels in loose connective tissue. Primordial follicles were typically found just below the tunica albuginea. Each one was made up of a layer of flat epithelial cells surrounding a primary ovum. Unilaminar primary follicles had an oocyte with a surrounding cuboidal layer of cells, and multilaminar primary follicles had an ovum circled with multiple laminae of follicular cells. Additionally, secondary follicles were present. Each secondary follicle consisted of multiple laminae of granulosa cells and several fluidic cavities. Tertiary follicles had a solitary antrum and their oocytes ringed with corona radiata and zona pellucida. Then theca folliculi cells encircled the follicle. Corpora lutea were filled with moderate eosinophilic cells with foamy cytoplasm. **Figures (1-4)**

The ovarian sections of Group 3 exhibited detachment of the germinal epithelium. There was a marked reduction in primordial follicles, limited normal ovarian follicles, and a prevalence of atretic follicles. The cells displayed fragmented and karyopyknotic nuclei. The cytoplasm appeared profoundly acidophilic. Additionally, disrupted zona pellucida surrounded some degenerated oocytes. Certain sections revealed tertiary follicles with nearly absent oocytes. Furthermore, vacuolated and profoundly eosinophilic were identified in degenerated corpora lutea. Prominent hyperemia with dilated, blood vessels was also observed. **Figures (5&6)**

The light microscopic examination of group IV displayed no correction in the ovarian tissue constitution. In this group, the germinal epithelium was in some sections detached from the

underlying tissue. Most of the follicles were atretic and with lost or degenerated oocytes. Dilated and congested blood vessels were detected. **Figures (7&8).**

The ovarian sections of groups V&VI revealed a nearly normal configuration of the ovaries as indicated by a decreased count of damaged follicles and a raised count of secondary and primary follicles. Several corpora lutea were also observed where the luteal cells displayed vesicular nuclei in moderately eosinophilic cytoplasm. However, dilated blood vessels were still detected. **Figures (9-12).**

### 3. 3. Immunohistochemical results

Evaluation of control groups sections displayed negative cytoplasmic and nuclear reactions in follicular, luteal, and vascular endothelial cells (**Figures 13&14**). Meanwhile, many follicular and luteal cells in group (III) showed intensely positive reactions. (**Figure 15**). In group (IV), the caspase-3 reaction was greatly positive (**Figure 16**). A dramatic decrease in caspase-3 activity in sections of groups V&VI was detected indicating normal follicular development as presented in (**Figures 17&18**).

**Table 1: Mean values ( $\pm$  SD) of serum MDA, TNF- $\alpha$ , SOD, and AMH levels in the studied groups.**

Groups Parameters	-ve control	+ve control	MTX	MTX+TQ1 2.5 mg/kg	MTX+TQ2 5mg/kg	MTX+TQ3 10mg/kg
MDA (nmol/ml)	4.63 $\pm$ .58	6.16 $\pm$ .97	30.53 $\pm$ 3.95 *acd	21.1 $\pm$ 3.14 *abd	10.46 $\pm$ 3.05 *bc	11.18 $\pm$ 3.31 *bc
TNF- $\alpha$ (Pg/ml)	36.4 $\pm$ 4.8	45.7 $\pm$ 6.6	115.9 $\pm$ 4.2 *ad	103.3 $\pm$ 6.1 *ad	73.2 $\pm$ 15.06 *abc	77.3 $\pm$ 11.4 *abc
SOD (U/ml)	159.03 $\pm$ 5.8	147.43 $\pm$ 10.8	55.1 $\pm$ 10.29 *ad	77.20 $\pm$ 6.69 *ad	114.58 $\pm$ 17.46 *abc	110.91 $\pm$ 15.26 *abc
AMH (ng/ml)	0.035 $\pm$ 0.004	0.035 $\pm$ 0.008	0.011 $\pm$ 0.001 *ad	0.015 $\pm$ 0.005 *ad	0.028 $\pm$ 0.0028 *bc	0.0267 $\pm$ 0.002 *bc

(\*) P value <0.05

(a) Significant P value when contrasted to control groups.

(b) Significant P value when contrasted to group III.

(c) Significant P value in contrast to group IV.

(d) Significant P value in contrast to groupsV &VI.

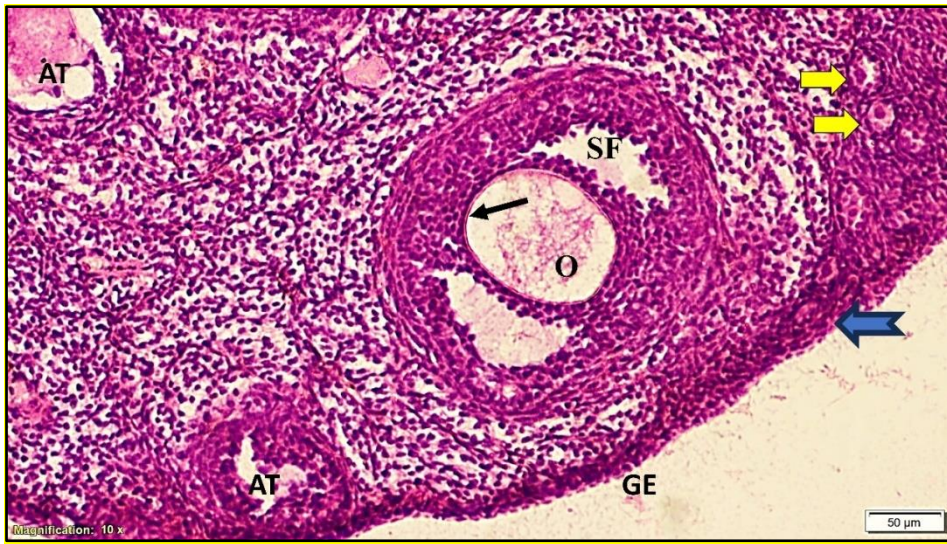


**Figure 1** photomicrograph of adult female albino rat ovarian section group (I) demonstrates normal tunica Albuginea (blue arrow), covered by a single germinal epithelium layer (GE). Primordial follicles (yellow arrows), a secondary follicle (SF) with zona pellucida (black arrow) encircling an oocyte (O), as well as a few atretic follicles (AT) are detected. (H&E X 100)

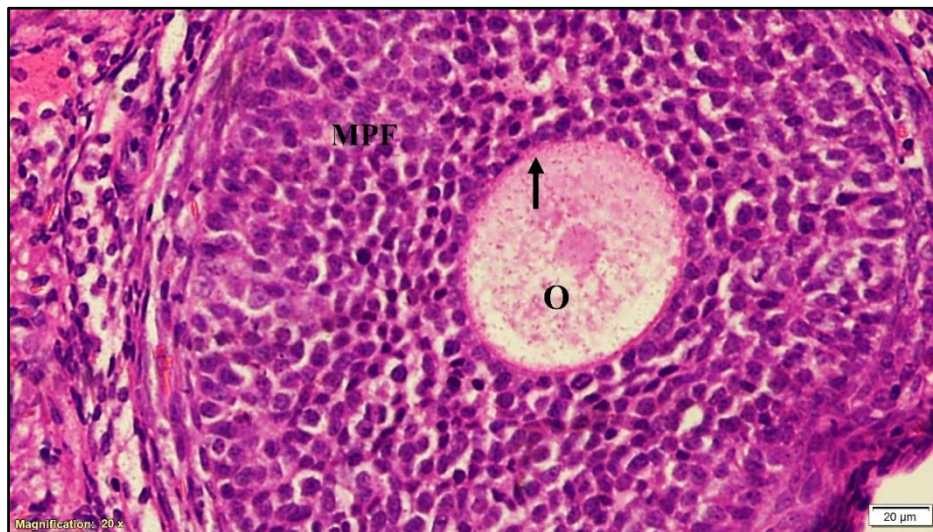


**Figure 2:** photomicrograph of adult female albino rat ovarian section group (I) demonstrates a multilaminar primary follicle (MPF) with an intact oocyte (O) surrounded by an acidophilic glycoprotein layer, zona pellucida, (arrow). (H&E X 200)

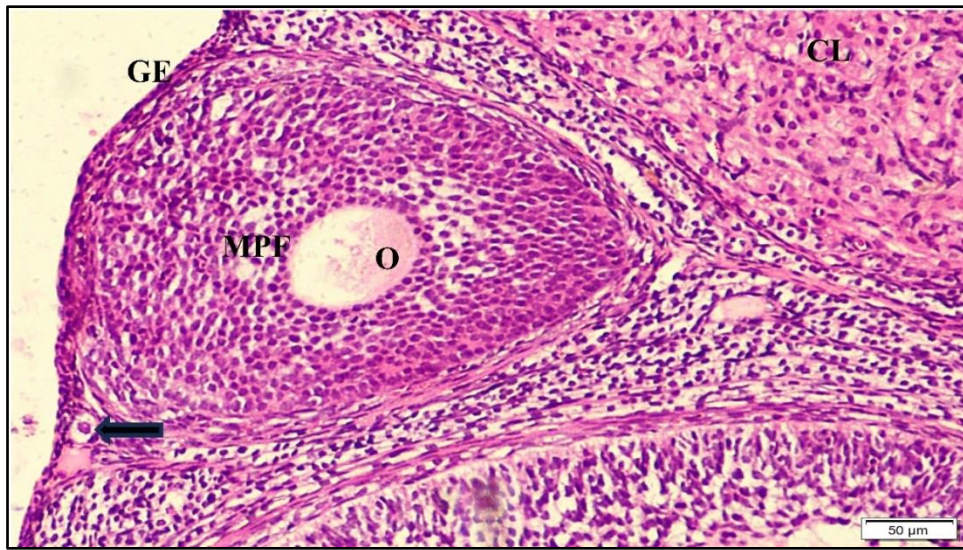


**Figure 3:** photomicrograph of adult female albino rat ovarian section group (II) demonstrates part of ovarian cortex covered by germinal epithelium (GE) and containing multilaminar primary follicle (MPF) with intact oocyte (O), a primordial follicle (arrow) and part of corpus luteum (CL) is also detected. (H&E X 100)

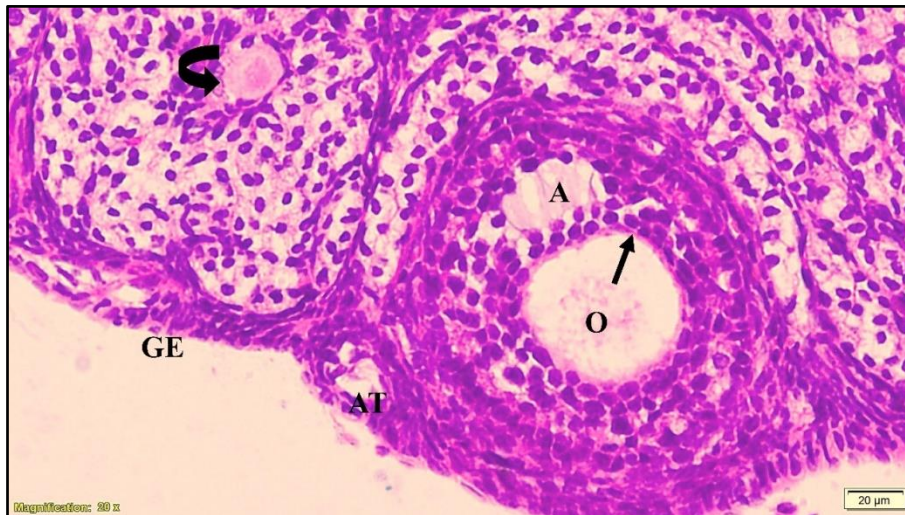


**Figure 4** photomicrograph of adult female albino rat ovarian section of group (II) showing the cortex covered with germinal Epithelium (GE), containing a secondary follicle with a small antrum (A), acidophilic zona pellucida (arrow) circling an intact oocyte (O). Unilaminar primordial follicle (curved arrow), and atretic follicle (AT) are detected. (H&E X 200)



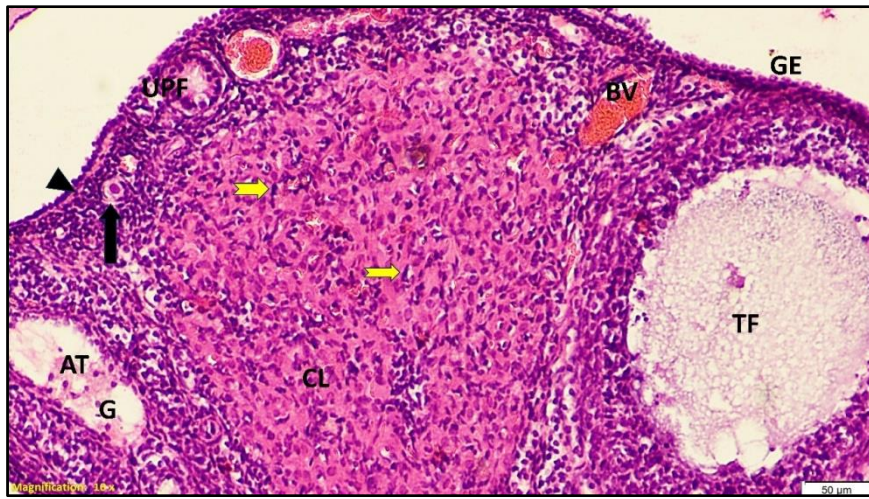


**Figure 5:** photomicrograph of adult female albino rat ovarian section group (III) showing tunica albuginea (arrowhead) beneath the germinal epithelium (GE) covering part of the cortex. The cortex shows degenerated tertiary follicle (TF) and atretic follicle (AT) with disturbed granulosa cells (G). A degenerated corpus luteum (CL) with cells that have deeply acidophilic cytoplasm and deeply stained nuclei (yellow arrows) as well as degenerated unilaminar primary follicle (UPF) are seen. A primordial follicle is also detected (black arrow). Evident dilated congested cortical blood vessels (BV) are seen. (H&E 100)

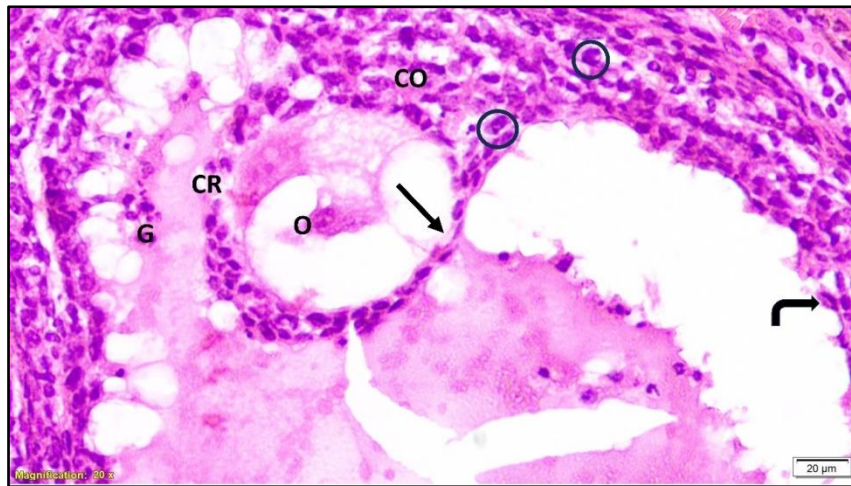


**Figure 6:** photomicrograph of adult female albino rat ovarian section rat group (III) demonstrates a degenerated preovulatory follicle with degenerated ova (O) and disrupted zona pellucida (straight arrow), disturbed corona radiata (CR), and cumulus oophorus (CO). Note the presence of apoptotic granulosa cells (G) with pycnotic nuclei (bent arrow) and fragmented nuclei (circles). (H&E 200)

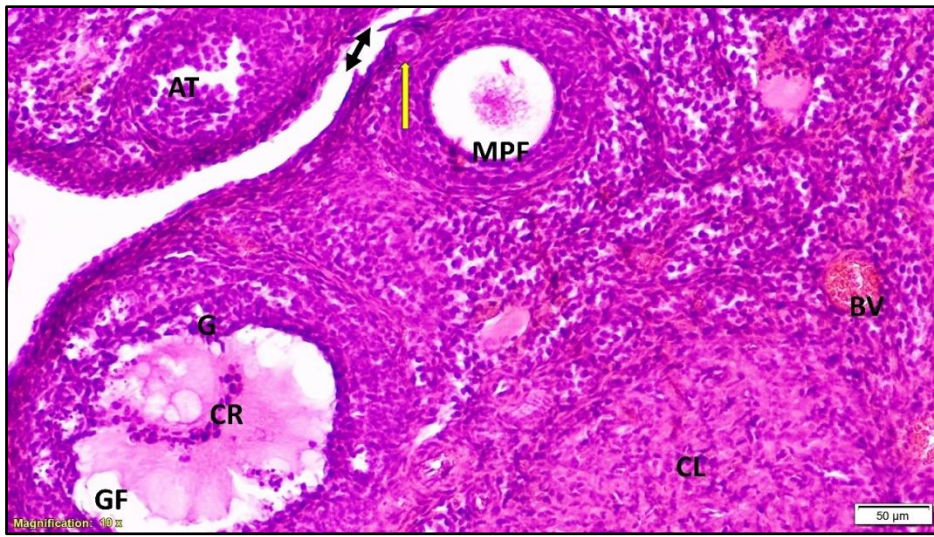


**Figure 7** photomicrograph of adult female albino rat ovarian section of group (IV) demonstrates detachment of germinal epithelium (black arrow). The cortex contains follicles at various stages of growth. A Primordial follicle (yellow arrow), a multilaminar primary follicle (MPF), and an atretic follicle (AT) are seen. A portion of corpus luteum (CL) and a deteriorated Graafian follicle (GF) with disturbed corona radiata (CR) and deeply stained granulosa cells (G) are detected. Blood vessels (BV) are dilated and congested. (H&E 100)

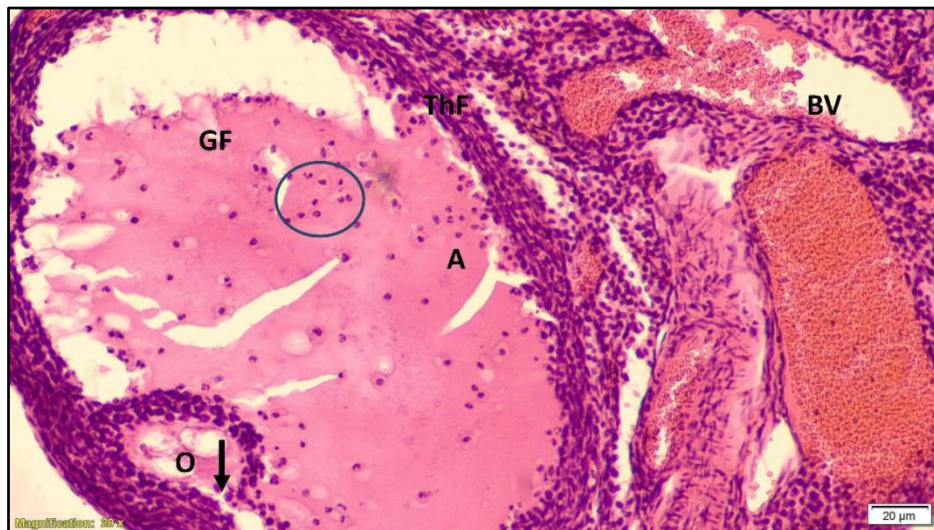


**Figure 8:** photomicrograph of adult female albino rat ovarian section group (IV) showing degenerated Graafian (GF) follicle with degenerated oocyte (O) and discontinuous corona radiata (arrow). Note the shedding granulosa cells (circle) into the antrum (A). A layer of Theca folliculi (ThF) surrounds the follicle. Blood vessels appeared markedly dilated and congested.(BV). (H&E 200)

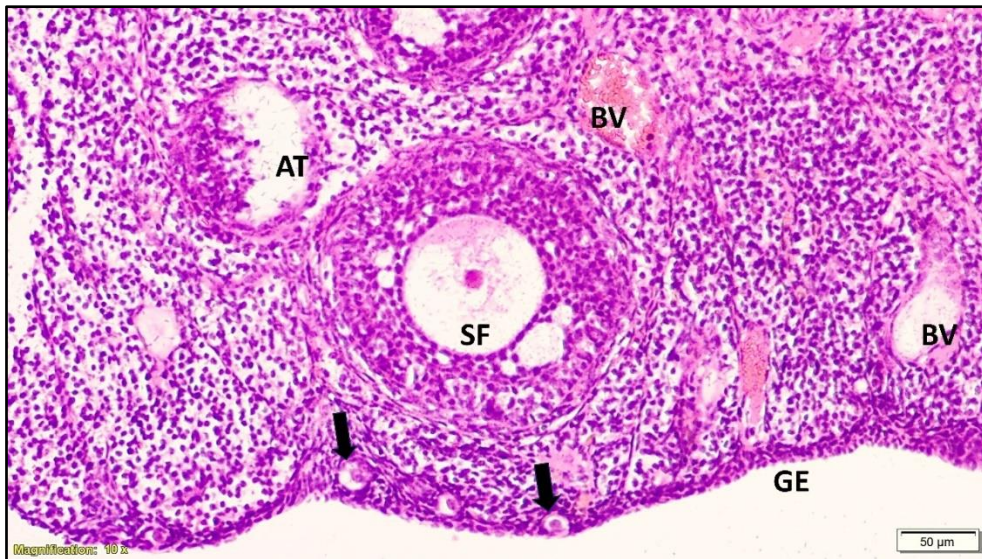


**Figure 9:** photomicrograph of adult female albino rat ovarian section group (V) demonstrates normal germinal epithelium (GE) covering part of the cortex where primordial follicles (arrows) are detected superficially. A secondary follicle (SF) and an atretic follicle (AT) are also seen. Cortical blood vessels (BV) appear dilated and congested. (H&E 100)

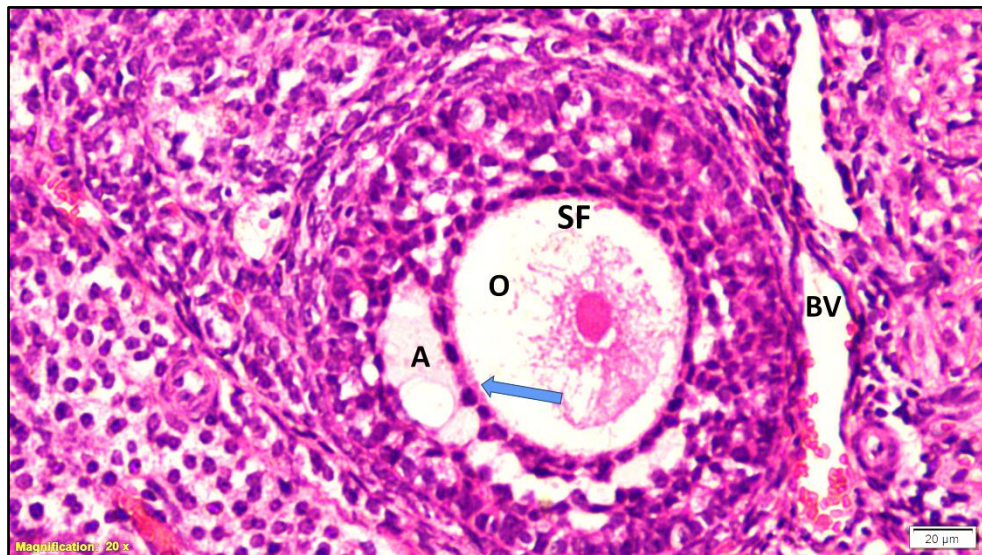


**Figure 10:** Photomicrograph of adult female albino rat ovarian section group (V) demonstrates a secondary follicle (SF) with an intact oocyte (O), a surrounding zona pellucida (arrow), and an antrum (A). Evident dilated congested blood vessels (BV) are detected. (H&E 200)

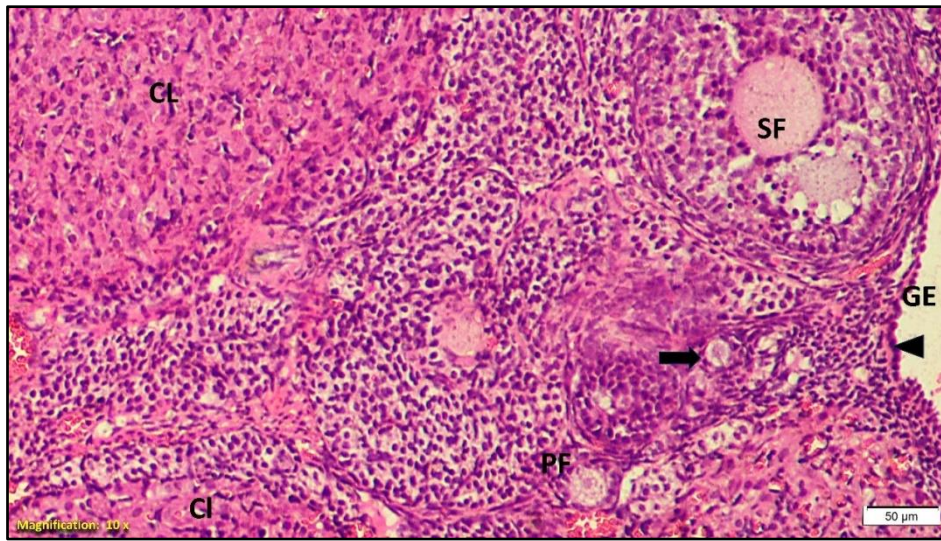


**Figure 11:** photomicrograph of adult female albino rat ovarian section group (VI) demonstrates normal tunica albuginea (arrowhead) underlying a layer of germinal epithelium (GE). The cortex shows almost normal follicles in various forms of growth and development. Primordial follicle (thick arrow), primary follicle (PF), and secondary follicle (SF) are seen. Multiple Corpora lutea (CL) are also detected. (H&E 100)

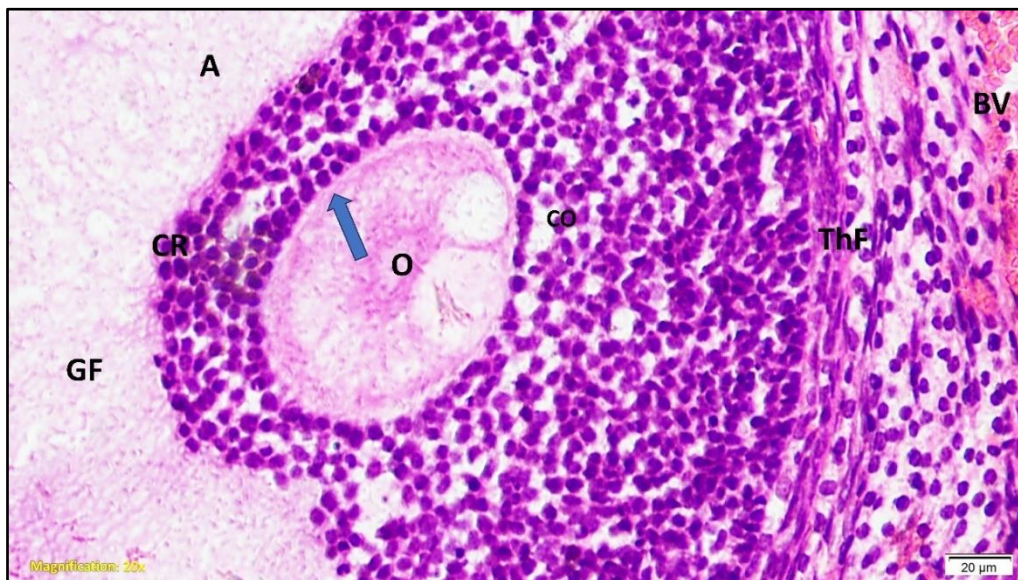


**Figure 12:** photomicrograph of adult female albino rat ovarian section group (VI) showing a Graafian follicle (GF) with a single antrum (A). It is formed of zona pellucida (arrow) surrounding an oocyte (O), cumulus oophorus (CO), and corona radiata (CR). Theca folliculi (ThF) surround the follicle. Dilated congested blood vessel (BV) is detected. (H&E X 200)

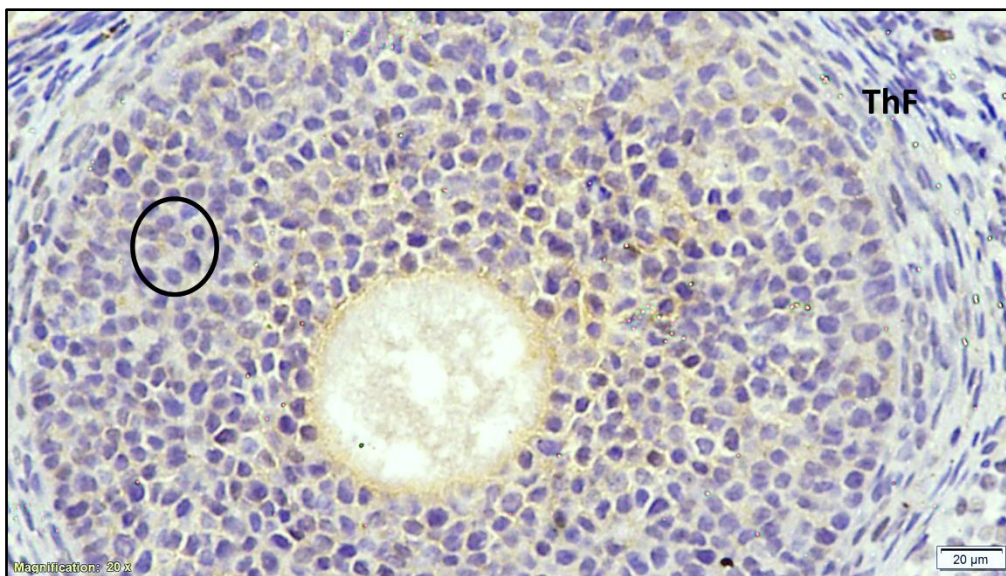


**Figure 13:** photomicrograph of adult female albino rat ovarian section group (I) demonstrates a negative caspase-3 immuno-activity in granulosa cells (circle) and theca cells (ThF) (Caspase-3 immunostaining X 200).

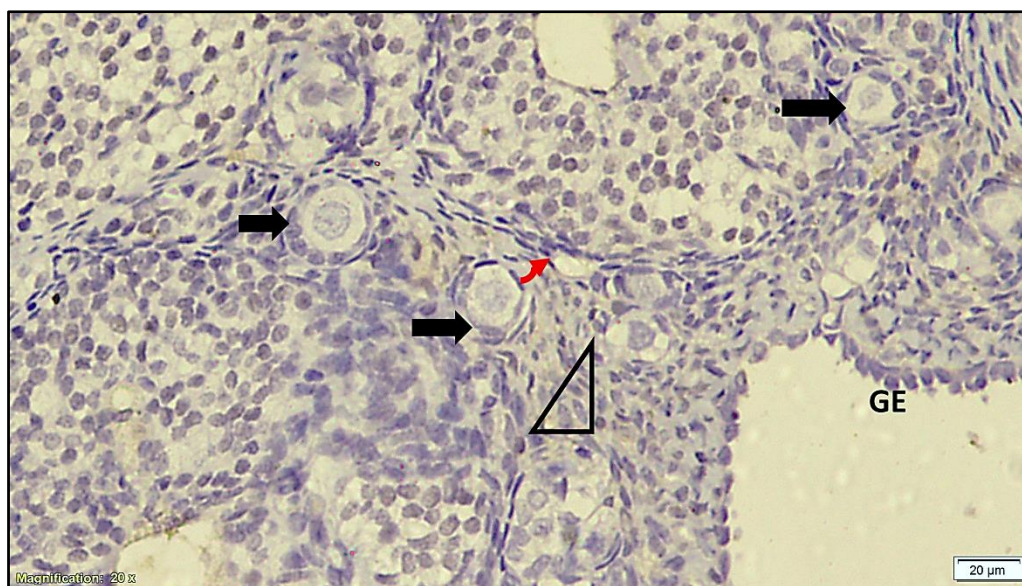


**Figure 14** photomicrograph of adult female albino rat ovarian section group (II) demonstrates a negative caspase-3 immuno-activity in follicular cells (black arrows), stromal cells (triangle), germinal epithelium (GE) and endothelial cells (red arrow). (Caspase-3 immunostaining X 200).

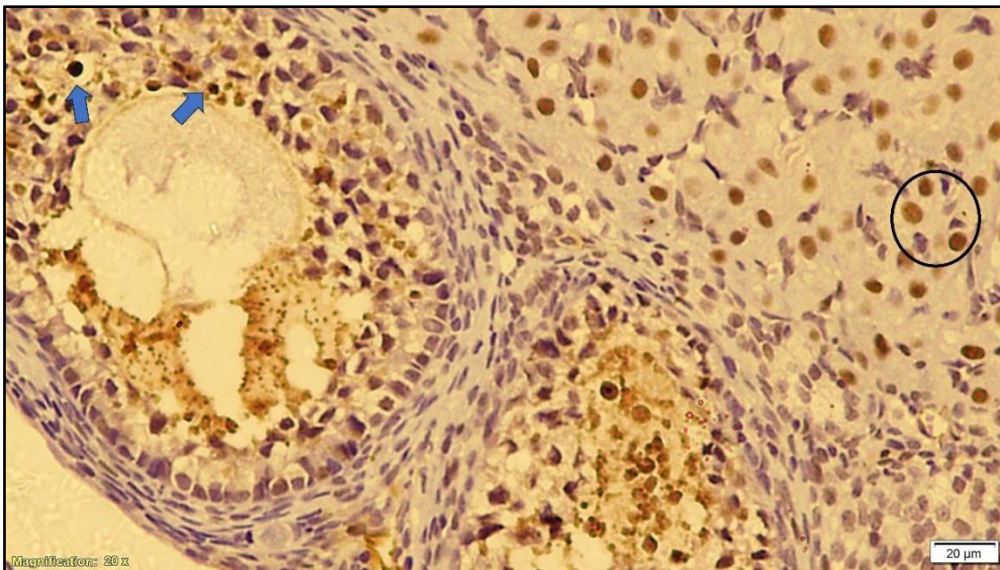


**Figure 15:** photomicrograph of adult female albino rat ovarian section group (III) demonstrates intense positive caspase-3 immuno-expression in follicular cells (arrows) as well as luteal cells of the corpus luteum (circle). (Caspase-3 immunostaining X 200).

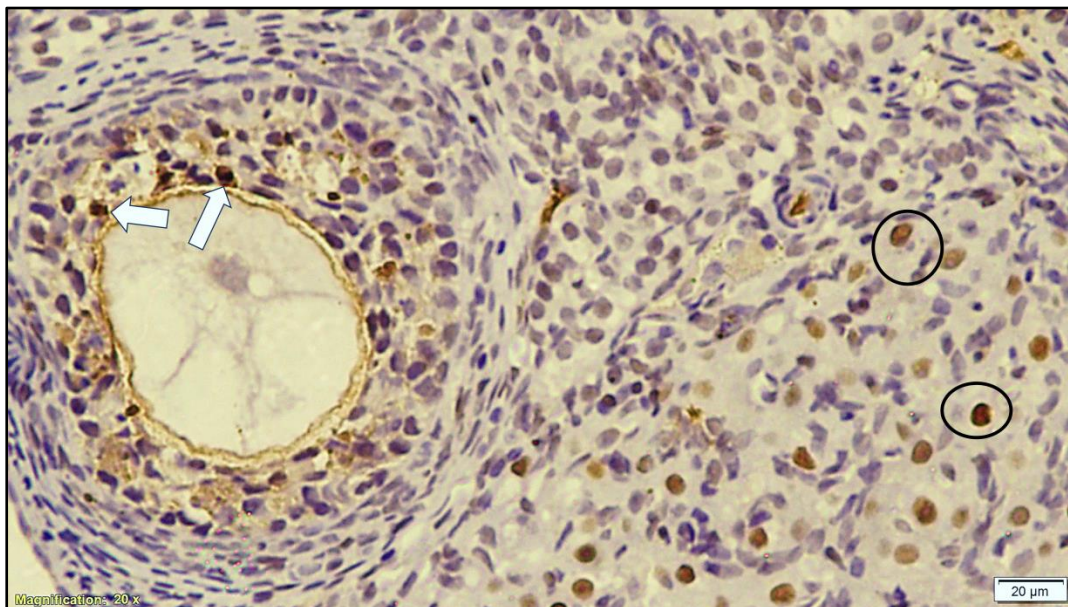


**Figure 16** photomicrograph of adult female albino rat ovarian section the group (IV) demonstrates positive caspase-3 immuno-expression in granulosa cells (arrows) as well as luteal cells (circles). (Caspase-3 immunostaining X 200)

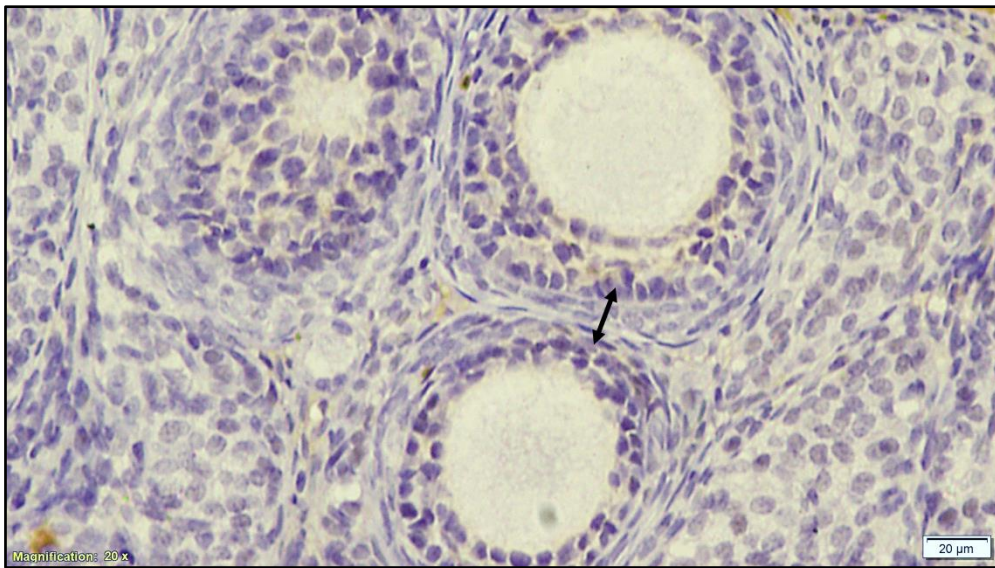


**Figure 17:** photomicrograph of adult female albino rat ovarian section group (V) demonstrates a negative caspase-3 immuno-activity in follicular cells (arrow). (Caspase-3 immunostaining X 200)

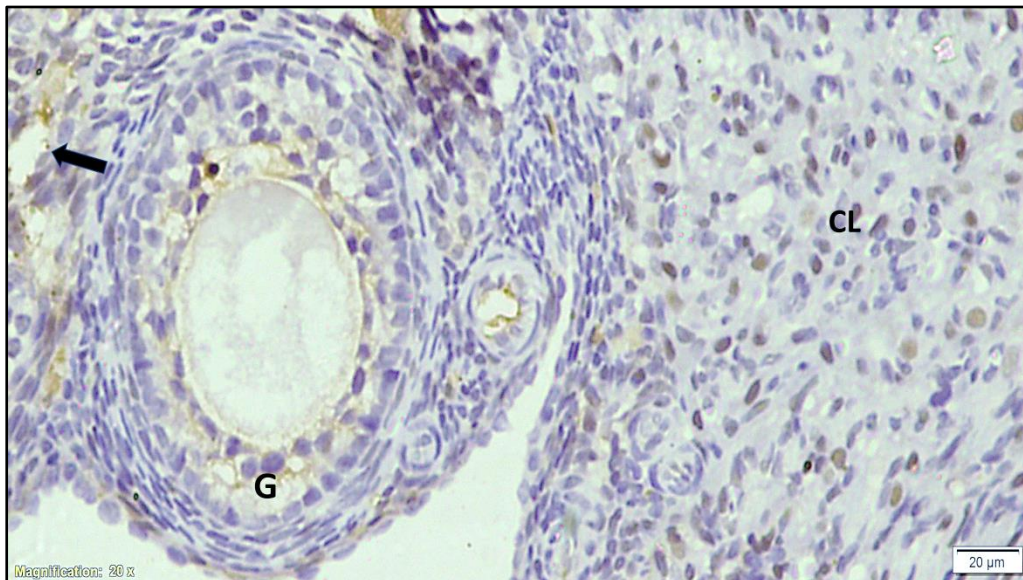


**Figure 18:** photomicrograph of adult female albino rat ovarian section group (VI) demonstrates negative caspase-3 immuno-expression in follicular granulosa cells (G), corpus luteum cells (CL), and vascular endothelial cells (arrow). (Caspase-3 immunostaining X 200)

#### 4. Discussion

Chemotherapy-induced toxicity targets different systems including the reproductive system. (Wang et al., 2020). While being frequently utilized as anti-cancer drug, MTX also causes multiple toxic effects on distinct systems of the body. Ali et al., 2014 and Madkour et al., 2022 stated that the underlying mechanisms involved in MTX toxicity are thought to be inflammation, apoptosis, and oxidative stress.

Thymoquinone, a natural biologically active drug extracted from *N. sativa*, has been approved to possess potent antioxidant activity as it serves as a scavenging agent of singlet

oxygen, superoxide and hydroxyl radicals. TQ's strong antioxidant effects are linked to the redox features of the quinone part of its structure, as well as its unhampered crossing of morphological barriers, thus freely accessing sub-cellular partitions and mitigating the reactive oxygen species (ROS). (Taysi et al., 2022). Therefore, TQ is an optimal subject to be investigated for its benefits in alleviating MTX's toxic effects on the ovaries.

Thus, this work aimed to study MTX's toxic impacts on the ovaries. Moreover, to evaluate the efficacy of different doses of TQ in ameliorating ovarian toxicity caused by MTX in female rats.

This work revealed remarkable changes in the biochemical parameters in MTX group compared to other groups.

the MTX group had a highly significant level of serum MDA, a product of lipid peroxidation. In accordance with this result, Soliman et al., 2020 reported a marked increase in serum MDA levels following oral administration of MTX in rats and explained liver and kidney damage caused by MTX by oxidative stress and lipid peroxidation. A similar finding was also reported by Alabdaly et al., 2021.

Xiong et al., 2019 and Eltamany et al., 2022 explained that the toxicity of MTX is related to profound oxidative stress mediated by ROS generation, and antioxidant defense system dysregulation.

The current study revealed a major reduction of serum SOD levels in methotrexate group versus the control groups. Sahindokuyucu-Kocasari et al., 2021 also reported a significant lower serum SOD level after intraperitoneal injection of MTX in rats and emphasized that MTX reduced the efficiency of the antioxidant systems causing liver and kidney toxicity.

A possible explanation for this could be that normally, ROS elimination is managed by a radical scavenging system, including glutathione reductase (GR), glutathione peroxidase, superoxide dismutase, glutathione and catalase, and The superoxide dismutase (SOD) regulates hydrogen peroxide and molecular oxygen generation from superoxide radical, then hydrogen peroxide converted into water and molecular oxygen by catalase, leading to a decrease in oxidative stress, thus protection of cells from damage. Slight changes in physiological concentrations of the enzymes may affect the resistance of DNA cellular proteins, lipids, and oxidative damage (Roghani et al., 2020 and Elsayy et al., 2021).

our study demonstrates that MTX caused a significant enhancement in serum inflammatory TNF- $\alpha$ . This was investigated by Elsayy et al., 2021 who declared that the generation of ROS induced by MTX leads to the upregulation of NF-Kb expression which is important for proinflammatory agents exemption like TNF- $\alpha$ , IL-6, nitric oxide synthase enzymes, which in turn aggravates the inflammatory response. Additionally, the proinflammatory agents facilitate immunological and inflammatory cell aggregation, such as neutrophils and macrophages, thus triggering ROS generation, exacerbating cellular damage and oxidative stress.

Studies of Hortu et al., 2020 and Madkour et al., 2022 announced that AMH levels were intensely reduced in MTX-treated animals compared to control group and this agrees with our results which showed the same findings.



**Madkour et al., 2022** stated that MTX ovarian toxicity leads to follicular, atresia, follicular apoptosis, and subsequently, a decrease in AMH level. **Çetin et al., 2022** explained that MTX may impair the blood flow and proliferation of the cells thus reducing ovarian reserve.

In our study, TQ (5&10 mg/kg) administration raised SOD levels and reduced the increased MDA levels significantly, suggesting its antioxidant properties.

**Al-Attar, 2022** revealed similar results and stated that TQ treatment markedly alleviated the hematological and biochemical effects in mice exposed to Thioacetamide, and the possible mechanism related to its anti-oxidant actions that were evaluated by the significant upregulation of SOD level.

**Yaghutian Nezhad et al., 2021** presented similar results and explained TQ's excellent antioxidant properties as it serves as a hydrogen atoms or electrons donor to reactive oxygen species that transforms into harmless compounds, and suppresses the lipid oxidation process.

**Alzohairy et al., 2021** declared that TQ reduced elevated TNF- $\alpha$  levels in rat exposed to lung toxicity and this result is in accordance with our study which demonstrates that treatment with TQ (5&10mg/kg) significantly decreased the TNF- $\alpha$  serum levels.

**Abdel-Daim et al., 2020** explained that TQ's ability to reduce the parameters of inflammation in acrylamide-treated rats may be due to oxidative stress counteracting or directly decreasing their expression levels.

The present study revealed that TQ treatment could counteract MTX-induced decrease in AMH levels. This is in harmony with **Sukatendel et al., 2021** results who demonstrated that Nigella sativa TQ-rich extract could alleviate Cisplatin ovarian toxicity

This could be explained by the fact that for increasing the viability of ovarian reserves, it's crucial to decrease levels of free radicals in the ovaries. Thymoquinone has a potent antioxidant activity which is reflected in the capacity to counteract superoxide anions and enhance the genes responsible for antioxidants generation such as SOD, Glutathione peroxidase and Catalase. (**Sukatendel et al., 2021**).

In the current study, TQ (2.5mg/kg) failed to make significant changes in the biochemical parameters compared to other groups of the study. This contrasts with **Fadishei et al., 2020** who showed that TQ (2mg/kg) significantly reduced serum level of TNF- $\alpha$  and interleukin-1 in rats treated by bisphenol A.

Histopathologic findings in the MTX group in this study revealed an intense loss in primordial follicles and a higher rise in atretic follicles with apoptotic cells. Furthermore, the zona pellucida around some degenerated oocytes was disrupted. Along with vascular congestion, which implies ovarian inflammation, there was mononuclear cell aggregation. There was vacuolation in follicular granulosa cells. Moreover, vacuolated, and profoundly eosinophilic cytoplasm with condensed nuclei were observed in degenerated corpora lutea.

These results agree with earlier studies of **Hussein, 2023, and Zhao et al., 2023** who reported disruption of normal ovarian epithelium, stromal fibrosis, an obvious decrease of primary and secondary follicles, cystic follicles, and polymorphs infiltrate as well as marked congestion in the stroma in the MTX-induced ovarian toxicity.

This outcome is anticipated in methotrexate-treated ovaries since the drug tends to cause cell apoptosis or hinder the cell cycle by increasing the generation of harmful reactive species as demonstrated by (AlBasher et al., 2018).

Here in, TQ administration dramatically diminished the severity of histopathological changes caused by MTX. However, TQ (5 and 10 mg/kg) reduced atretic follicle count and elevated corpora lutea, primary follicles, antral follicles, and Graafian follicles quantity in treated animals.

our results are similar to Alaei et al. (2022) who studied TQ effect on letrozole- ovarian toxicity. Treating rats with doses of 5 & 10 mg/kg could decrease atretic follicles count, improve multilaminar and antral follicle count, and restore normal ovulation in female rats. Additionally, Al-Ghamdi et al. (2023) reported that TQ could restore the degenerative changes in the ovaries of female rats treated with acrylamide.

In our study, immunohistochemical staining with caspase 3 showed increased expression in ovarian sections treated with MTX. Bašković & Ježek, 2022 and Zhao et al., 2023 also reported increased caspase 3 expression in MTX-induced ovarian injury.

In addition, apoptosis had a key role in MTX toxicity. Zhao et al., 2023 explained that cytochrome c release into the cytosol stimulates caspase 3, a significant apoptotic marker. The caspase cascade stimulation causes the disintegration of the nucleus and cellular degeneration.

This study revealed that treatment with TQ (5&10 mg/kg) notably attenuated ovarian caspase 3 activity, in coincide with Zakzook et al., 2020 who declared a marked reduction in expression of caspase3 in testicular tissues of dimethoate-exposed rats following treatment with TQ 10mg/kg by oral gavage and explained that the following mechanisms could be responsible for TQ's anti-apoptotic effects: antioxidant action, immunomodulatory effect, and genoprotective potential by enhancing the genes responsible for the recognition and repair of damaged DNA.

However, our results revealed that TQ (2.5mg/kg) failed to decrease caspase-3 immun-expression in the ovarian sections. Firdaus et al., 2018 also demonstrated that TQ (2.5mg/kg) failed to decrease caspase-3 level however TQ (5mg/kg) was able to decrease it implying the beneficial dose-dependent anti-apoptotic effect of TQ.

It is worth noting that TQ has dose-dependent protective effects because the beneficial effects of the doses (5 and 10 mg/ kg) in minimizing MTX implications on indicators of oxidative stress and reconstruction of ovarian tissue were more remarkable compared to (2.5 mg/kg) dose.

Mehri et al., 2014 searched TQ (2.5, 5 &10mg/kg) effect in acrylamide- neurotoxicity in rats. (2.5 mg/kg)of TQ caused an insignificant decrease in MDA level in contrast to TQ (5 &10 mg/kg) which enhanced MDA level, body weight, and gait scores compared to acrylamide-treated rats.

Furthermore, Yaghutian Nezhad et al., 2021 assumed that TQ's protective properties on the reproductive organs are linked to administration dosage. For instance, 7.5 mg/kg TQ was more capable than 15 mg/kg to lower bleomycin implications on biomarkers of male fertility.

## Conclusion

We concluded that Thymoquinone could reverse methotrexate's toxic effects on ovarian function and structure. This work revealed that MTX exerted toxic impacts on the ovaries of female rats as evidenced by the raised MDA and TNF- $\alpha$  levels, decreased SOD activity and AMH levels, and increased caspase-3 immuno-expression as well as histopathological changes in the ovarian tissue. Meanwhile, thymoquinone treatment markedly counteracted these effects. TQ's beneficial properties are linked to antioxidant, anti-apoptotic and anti-inflammatory ability. Thus, thymoquinone could be counted for counteracting MTX toxicities. Additional research is needed to elucidate the precise methods of action mediating the beneficial effects of TQ in ovarian damage caused by MTX. More research should be done to observe the impact of higher doses and longer duration of thymoquinone on ovarian tissue.

## References

1. Abdel-Daim, M. M., Abo El-Ela, F. I., Alshahrani, F. K., Bin-Jumah, M., Al-Zharani, M., Almutairi, B., Alyousif, M. S., Bungau, S., Aleya, L., & Alkahtani, S. (2020). Protective effects of thymoquinone against acrylamide-induced liver, kidney and brain oxidative damage in rats. *Environmental science and pollution research international*, 27(30), 37709–37717. <https://doi.org/10.1007/s11356-020-09516-3>
2. Alabdaly, Yamama, Saeed, M., & Al-hashemi, H. (2021). Effect of methotrexate and aspirin interaction and its relationship to oxidative stress in rats. *Iraqi Journal of Veterinary Sciences*, 35(1), 151–156. <https://doi.org/10.33899/ijvs.2020.126490.1335>
3. Alabdullah, S. W., Alsamir, S. A., & AlRufaei, I. A. (2020). Effect of Thymoquinone on some biochemical and hormonal indices and their protective effect on the genital organs of rats after cancer induction in Laboratory. *EurAsian J. BioSci*, 14, 567-573.
4. Alae, S., Mirani, M., Derakhshan, Z., Koohpeyma, F., & Bakhtari, A. (2023). Thymoquinone improves folliculogenesis, sexual hormones, gene expression of apoptotic markers and antioxidant enzymes in polycystic ovary syndrome rat model. *Veterinary medicine and science*, 9(1), 290–300. <https://doi.org/10.1002/vms3.958>
5. Al-Attar A. M. (2022). Hematological and biochemical investigations on the effect of curcumin and Thymoquinone in male mice exposed to Thioacetamide. *Saudi journal of biological sciences*, 29(1), 660–665. <https://doi.org/10.1016/j.sjbs.2021.10.037>
6. AlBasher, G., AlKahtane, A. A., Alarifi, S., Ali, D., Alessia, M. S., Almeer, R. S., Abdel-Daim, M. M., Al-Sultan, N. K., Al-Qahtani, A. A., Ali, H., & Alkahtani, S. (2018). Methotrexate-induced apoptosis in human ovarian adenocarcinoma SKOV-3 cells via ROS-mediated bax/bcl-2-cyt-c release cascading. *OncoTargets and therapy*, 12, 21–30. <https://doi.org/10.2147/OTT.S178510>
7. Al-Ghamdi, M., Huwait, E., ElSawi, N., Shaker Ali, S., & Sayed, A. (2023). Thymoquinone ameliorates acrylamide-induced reproductive toxicity in female rats: An experimental study. *International journal of reproductive biomedicine*, 21(1), 61–70. <https://doi.org/10.18502/ijrm.v21i1.12668>
8. Ali, N., Rashid, S., Nafees, S., Hasan, S. K., & Sultana, S. (2014). Beneficial effects of Chrysin against Methotrexate-induced hepatotoxicity via attenuation of oxidative stress and apoptosis. *Molecular and cellular biochemistry*, 385(1-2), 215–223. <https://doi.org/10.1007/s11010-013-1830-4>
9. Alzohairy, M. A., Khan, A. A., Alsahli, M. A., Almatroodi, S. A., & Rahmani, A. H. (2021). Protective Effects of Thymoquinone, an Active Compound of Nigella sativa,

- on Rats with Benzo(a)pyrene-Induced Lung Injury through Regulation of Oxidative Stress and Inflammation. *Molecules (Basel, Switzerland)*, 26(11), 3218. <https://doi.org/10.3390/molecules26113218>
10. Bajas, D., Vlase, G., Mateescu, M., Grad, O. A., Bunoiu, M., Vlase, T., & Avram, C. (2021). Formulation and Characterization of Alginate-Based Membranes for the Potential Transdermal Delivery of Methotrexate. *Polymers*, 13(1), 161. <https://doi.org/10.3390/polym13010161>
  11. Bašković, M., & Ježek, D. (2022). Methotrexate-induced toxic effects and the ameliorating effects of astaxanthin on genitourinary tissues in a female rat model. *Archives of gynecology and obstetrics*, 306(6), 2199–2200. <https://doi.org/10.1007/s00404-022-06488-2>
  12. Bedoui, Y., Guillot, X., Sélambarom, J., Guiraud, P., Giry, C., Jaffar-Bandjee, M. C., Ralandison, S., & Gasque, P. (2019). Methotrexate an Old Drug with New Tricks. *International journal of molecular sciences*, 20(20), 5023. <https://doi.org/10.3390/ijms20205023>
  13. Çetin, F., Bayramoglu Tepe, N., & Kutlar, A. I. (2023). Evaluation of the effect of multi-dose methotrexate therapy on ovarian reserve in ectopic pregnancies: is polycystic ovarian morphology a protective condition for ovarian reserve?. *Ginekologia polska*, 94(5), 407–414. <https://doi.org/10.5603/GP.a2022.0077>
  14. Colluoglu, C., Balci, S., GÜNDOĞDU, B., ÇOBAN, T., Bulut, S., & SÜLEYMAN, H. (2022). Effect of thymoquinone on cyclophosphamide-induced oxidative and inflammatory ovarian damage in rat. *Bangladesh Journal of Pharmacology*, 17(3). <https://doi.org/10.3329/bjp.v17i3.59418>
  15. Cronstein, B. N., & Aune, T. M. (2020). Methotrexate and its mechanisms of action in inflammatory arthritis. *Nature reviews. Rheumatology*, 16(3), 145–154. <https://doi.org/10.1038/s41584-020-0373-9>
  16. El-Fatah, M. D. M. Y. S. S. A., & Alsemeh, A. E. (2019). Oxidative stress changes induced by methotrexate on parotid gland structure of adult male albino rat: Can vitamin C ameliorate these changes? *The Medical Journal of Cairo University, the Medical Journal of Cairo University*, 87(June), 2555–2565. <https://doi.org/10.21608/mjcu.2019.54869>
  17. Elsayy, H., Alzahrani, A. M., Alfwuaires, M., Abdel-Moneim, A. M., & Khalil, M. (2021). Nephroprotective effect of naringin in methotrexate induced renal toxicity in male rats. *Biomedicine & pharmacotherapy = Biomedecine & pharmacotherapie*, 143, 112180. <https://doi.org/10.1016/j.biopha.2021.112180>
  18. Eltamany, E. E., Mosalam, E. M., Mehanna, E. T., Awad, B. M., Mosaad, S. M., Abdel-Kader, M. S., Ibrahim, A. K., Badr, J. M., & Goda, M. S. (2022). Potential Gonado-Protective Effect of *Cichorium endivia* and Its Major Phenolic Acids against Methotrexate-Induced Testicular Injury in Mice. *Biomedicines*, 10(8), 1986. <https://doi.org/10.3390/biomedicines10081986>
  19. Fadishei, M., Ghasemzadeh Rahbardar, M., Imenshahidi, M., Mohajeri, A., Razavi, B. M., & Hosseinzadeh, H. (2021). Effects of Nigella sativa oil and thymoquinone against bisphenol A-induced metabolic disorder in rats. *Phytotherapy research : PTR*, 35(4), 2005–2024. <https://doi.org/10.1002/ptr.6944>
  20. Farooq, J., Sultana, R., Taj, T., Asdaq, S. M. B., Alsalman, A. J., Mohaini, M. A., Al Hawaj, M. A., Kamal, M., Alghamdi, S., Imran, M., Shahin, H., & Tabassum, R. (2021). Insights into the Protective Effects of Thymoquinone against Toxicities Induced by Chemotherapeutic Agents. *Molecules (Basel, Switzerland)*, 27(1), 226. <https://doi.org/10.3390/molecules27010226>

21. Firdaus, F., Zafeer, M. F., Waseem, M., Ullah, R., Ahmad, M., & Afzal, M. (2018). Thymoquinone alleviates arsenic induced hippocampal toxicity and mitochondrial dysfunction by modulating mPTP in Wistar rats. *Biomedicine & pharmacotherapy = Biomedecine & pharmacotherapie*, *102*, 1152–1160. <https://doi.org/10.1016/j.biopha.2018.03.159>
22. Gunyeli, I., Saygin, M., & Ozmen, O. (2021). Methotrexate-induced toxic effects and the ameliorating effects of astaxanthin on genitourinary tissues in a female rat model. *Archives of gynecology and obstetrics*, *304*(4), 985–997. <https://doi.org/10.1007/s00404-021-06000-2>
23. Hafez, S. M. N. A., Elbassuoni, E., Abdelzاهر, W. Y., Welson, N. N., Batiha, G. E., Alzahrani, K. J., & Abdelbaky, F. A. F. (2021). Efficacy of vitamin E in protection against methotrexate induced placental injury in albino rats. *Biomedicine & pharmacotherapy = Biomedecine & pharmacotherapie*, *139*, 111637. <https://doi.org/10.1016/j.biopha.2021.111637>
24. Hortu, I., Ozceltik, G., Ergenoglu, A. M., Yigitturk, G., Atasoy, O., & Erbas, O. (2020). Protective effect of oxytocin on a methotrexate-induced ovarian toxicity model. *Archives of gynecology and obstetrics*, *301*(5), 1317–1324. <https://doi.org/10.1007/s00404-020-05534-1>
25. Hussein, A., & Ali, S. M. (2022). A short-term comparison between the effect of two different concentrations of methotrexate on ovarian tissues and function of female albino rats. *Journal of the Faculty of Medicine Baghdad*, *64*(4), 280–285. <https://doi.org/10.32007/jfacmedbagdad.6441967>
26. Aka, K. K., Acar, I. A., Özgöçmen, M., Aslankoç, R., & Yeşilot, K. (2022). RESVERATROL ALLEVIATES METHOTREXATE-INDUCED OVARIAN INJURY VIA SUPPRESSING OXIDATIVE STRESS AND APOPTOSIS IN RATS. *Medical Journal of Suleyman Demirel University*, *29*(3), 476484. <https://doi.org/10.17343/sdutfd.1145034>
27. Laferriere, C. A., & Pang, D. S. J. (2020). Review of Intraperitoneal Injection of Sodium Pentobarbital as a Method of Euthanasia in Laboratory Rodents. *Journal of the American Association for Laboratory Animal Science: JAALAS*, *59*(3), 343. <https://doi.org/10.30802/AALAS-JAALAS-19-000081>
28. Mammadov, R., Suleyman, B., Akturan, S., Cimen, F. K., Kurt, N., Suleyman, Z., & Malkoc, İ. (2019). Effect of lutein on methotrexate-induced oxidative lung damage in rats: a biochemical and histopathological assessment. *The Korean journal of internal medicine*, *34*(6), 1279–1286. <https://doi.org/10.3904/kjim.2018.145>
29. Mehri, S., Shahi, M., Razavi, B. M., Hassani, F. V., & Hosseinzadeh, H. (2014). Neuroprotective effect of thymoquinone in acrylamide-induced neurotoxicity in Wistar rats. *Iranian journal of basic medical sciences*, *17*(12), 1007–1011.
30. Mikhaylov, D., Hashim, P. W., Nektalova, T., & Goldenberg, G. (2019). Systemic Psoriasis Therapies and Comorbid Disease in Patients with Psoriasis: A Review of Potential Risks and Benefits. *The Journal of clinical and aesthetic dermatology*, *12*(6), 46–54.
31. Nishikimi, M., Appaji, N., & Yagi, K. (1972). The occurrence of superoxide anion in the reaction of reduced phenazine methosulfate and molecular oxygen. *Biochemical and biophysical research communications*, *46*(2), 849–854. [https://doi.org/10.1016/s0006-291x\(72\)80218-3](https://doi.org/10.1016/s0006-291x(72)80218-3)
32. Patel, N., Shrivastava, R., & Shrivastava, V. K. (2023). Ameliorative role of thymoquinone against reprotoxic effect caused by potassium bromate in female mice. *Comparative Clinical Pathology*, *32*(3), 467–475. <https://doi.org/10.1007/s00580-023-03458-1>

33. Roghani, M., Kalantari, H., Khodayar, M. J., Khorsandi, L., Kalantar, M., Goudarzi, M., & Kalantar, H. (2020). Alleviation of Liver Dysfunction, Oxidative Stress and Inflammation Underlies the Protective Effect of Ferulic Acid in Methotrexate-Induced Hepatotoxicity. *Drug design, development and therapy*, *14*, 1933–1941. <https://doi.org/10.2147/DDDT.S237107>
34. Sahindokuyucu-Kocasari, F., Akyol, Y., Ozmen, O., Erdemli-Kose, S. B., & Garli, S. (2021). Apigenin alleviates methotrexate-induced liver and kidney injury in mice. *Human & experimental toxicology*, *40*(10), 1721–1731. <https://doi.org/10.1177/09603271211009964>
35. Kei, S. (1978). Serum lipid peroxide in cerebrovascular disorders determined by a new colorimetric method. *Clinica chimica acta*, *90*(1), 37-43.
36. Singh, R. K., van Haandel, L., Kiptoo, P., Becker, M. L., Siahaan, T. J., & Funk, R. S. (2019). Methotrexate disposition, anti-folate activity and efficacy in the collagen-induced arthritis mouse model. *European journal of pharmacology*, *853*, 264–274. <https://doi.org/10.1016/j.ejphar.2019.03.052>
37. Soliman, M. M., Aldhahrani, A., Alkhedaide, A., Nassan, M. A., Althobaiti, F., & Mohamed, W. A. (2020). The ameliorative impacts of Moringa oleifera leaf extract against oxidative stress and methotrexate-induced hepato-renal dysfunction. *Biomedicine & pharmacotherapy = Biomedecine & pharmacotherapie*, *128*, 110259. <https://doi.org/10.1016/j.biopha.2020.110259>
38. Sukatendel, K., Siregar, M. F. G., Natadisastra, M., Nasution, I. P. A., Ilyas, S., Tala, M. R., ... & Hasibuan, P. A. Z. (2021). Benefits of Nigella sativa extract protecting ovary due to Cisplatin chemotherapy. *Open Access Macedonian Journal of Medical Sciences*, *9*(A), 680-687. <https://doi.org/10.3889/oamjms.2021.6446>
39. Tabassum, S., Rosli, N., Ichwan, S. J. A., & Mishra, P. (2021). Thymoquinone and its pharmacological perspective: A review. *Pharmacological Research-Modern Chinese Medicine*, *1*, 100020.
40. Taysi, S., Algburi, F. S., Mohammed, Z. R., Ali, O. A., & Taysi, M. E. (2022). Thymoquinone: A Review on its Pharmacological Importance, and its Association with Oxidative Stress, COVID-19, and Radiotherapy. *Mini reviews in medicinal chemistry*, *22*(14), 1847–1875. <https://doi.org/10.2174/1389557522666220104151225>
41. Wang, L., He, Y., Li, Y., Pei, C., Olatunji, O. J., Tang, J., Famurewa, A. C., Wang, H., & Yan, B. (2020). Protective Effects of Nucleosides-Rich Extract from Cordyceps cicadae against Cisplatin Induced Testicular Damage. *Chemistry & biodiversity*, *17*(11), e2000671. <https://doi.org/10.1002/cbdv.202000671>
42. Xiong, S., Song, D., Xiang, Y., Li, Y., Zhong, Y., Li, H., Zhang, P., Zhou, W., Zeng, X., & Zhang, X. (2020). Reactive oxygen species, not Ca<sup>2+</sup>, mediates methotrexate-induced autophagy and apoptosis in spermatocyte cell line. *Basic & clinical pharmacology & toxicology*, *126*(2), 144–152. <https://doi.org/10.1111/bcpt.13306>
43. Yaghutian Nezhad, L., Mohseni Kouchesfahani, H., Alaei, S., & Bakhtari, A. (2021). Thymoquinone ameliorates bleomycin-induced reproductive toxicity in male Balb/c mice. *Human & experimental toxicology*, *40*(12\_suppl), S611–S621. <https://doi.org/10.1177/09603271211048184>
44. Zaki, S. M., Hussein, G. H. A., Khalil, H. M. A., & Abd Algaleel, W. A. (2021). Febuxostat ameliorates methotrexate-induced lung damage. *Folia morphologica*, *80*(2), 392–402. <https://doi.org/10.5603/FM.a2020.0075>
45. Zakzook, F., Hegazy, H., Yosef, T., & Gomaa, G. (2020). Thymoquinone attenuates dimethoate induced hepatic and testicular genotoxicity in rats. *Kafrelsheikh Veterinary Medical Journal*, *18*(2), 25-32. <https://doi.org/10.21608/kvmj.2020.40514.1010>

46. Zhao, L. L., Jayeoye, T. J., Ashaolu, T. J., & Olatunji, O. J. (2023). Pinostrobin, a dietary bioflavonoid exerts antioxidant, anti-inflammatory, and anti-apoptotic protective effects against methotrexate-induced ovarian toxicity in rats. *Tissue & cell*, 85, 102254. <https://doi.org/10.1016/j.tice.2023.102254>